Glycogen Synthase Kinase 3 Regulates Cell Death and Survival Signaling in Tumor Cells under Redox Stress[1]

Roberta Venè*, Barbara Cardinali*, Giuseppe Arena*, Nicoletta Ferrari*, Roberto Benelli*, Simona Minghelli*, Alessandro Poggi*, Douglas M. Noonan[†,‡], Adriana Albini[§,] and Francesca Tosetti*,

*IRCCS Azienda Ospedaliera Universitaria S. Martino-IST Istituto Nazionale per la Ricerca sul Cancro, Genova 16132, Italy; [†]Dipartimento di Biotecnologie e Scienze della Vita, Università degli Studi dell'Insubria, Varese 21100, Italy; [‡]Science and Technology Pole, IRCCS MultiMedica, Milan 20138, Italy; [§]Infrastruttura Ricerca-Statistica (I-RS), IRCCS Tecnologie Avanzate e Modelli Assistenziali in Oncologia, Arcispedale S. Maria Nuova, Reggio Emilia 42123, Italy

Abstract

Targeting tumor-specific metabolic adaptations is a promising anticancer strategy when tumor defense mechanisms are restrained. Here, we show that redox-modulating drugs including the retinoid N-(4-hydroxyphenyl)retinamide (4HPR), the synthetic triterpenoid bardoxolone (2-cyano-3,12-dioxooleana-1,9(11)-dien-28-oic acid methyl ester), arsenic trioxide (As_2O_3), and phenylethyl isothiocyanate (PEITC), while affecting tumor cell viability, induce sustained Ser9 phosphorylation of the multifunctional kinase glycogen synthase kinase 3β (GSK3β). The antioxidant N-acetylcysteine decreased GSK3β phosphorylation and poly(ADP-ribose) polymerase cleavage induced by 4HPR, As_2O_3, and PEITC, implicating oxidative stress in these effects. GSK3β phosphorylation was associated with up-regulation of antioxidant enzymes, in particular heme oxygenase-1 (HO-1), and transient elevation of intracellular glutathione (GSH) in cells surviving acute stress, before occurrence of irreversible damage and death. Genetic inactivation of GSK3β or transfection with the non-phosphorylatable GSK3β-S9A mutant inhibited HO-1 induction under redox stress, while tumor cells resistant to 4HPR exhibited increased GSK3β phosphorylation, HO-1 expression, and GSH levels. The above-listed findings are consistent with a role for sustained GSK3β phosphorylation in a signaling network activating antioxidant effector mechanisms during oxidoreductive stress. These data underlie the importance of combination regimens of antitumor redox drugs with inhibitors of survival signaling to improve control of tumor development and progression and overcome chemoresistance.

Neoplasia (2014) 16, 710–722

Introduction

Recent innovative approaches to cancer chemoprevention and treatment focus on tumor-specific metabolic adaptations as drug targets. In particular, some redox drugs appear to deeply compromise tumor bioenergetics [1]. Antitumor agents belonging to this class of chemicals, including the chemopreventive agent N-(4-hydroxyphenyl)retinamide (4HPR) [2], the synthetic triterpenoid 2-cyano-3,12-dioxooleana-1,9(11)-dien-28-oic acid methyl ester (CDDO-Me; RTA402 or bardoxolone methyl) [3], and phytochemicals such as phenylethyl isothiocyanate (PEITC) [4], are under scrutiny in clinical studies. Accordingly, patterns of the antioxidant machinery are currently used as biomarkers in clinical trials for metabolic disorders and cancer.

The main cytoprotective pathways against cell death originate from growth factor–activated phosphatidylinositol 3-kinase and AKT and by transient activation of the mitogen-activated protein kinase p42/p44 MAPK (ERK1/2) through ras-mediated pathways. These signaling molecules, and related transcription factors, are of a stress-sensing network that can modify the activity and expression of effectors involved in redox homeostasis, in concert with modulation of glutathione (GSH) metabolism and the activation of a battery of antioxidant enzymes [5]. The multifunctional glycogen synthase kinase 3β (GSK3β) is a key convergence point of survival pathways mediated by Ser/Thr protein kinases most related to PKA, PKG, PKC (AGC) kinases (AKT, protein kinase C (PKC), and cAMP-dependent protein kinase (PKA)), ERK1/2, and Wnt. Accordingly, GSK3β inhibitors are under clinical scrutiny in both neurodegenerative disorders and in cardioprotection. GSK3β activity depends on the balance between the activating Tyr216 phosphorylation and the inactivating phosphorylation at Ser9. Recent evidence indicates that active GSK3β in tumors can be proapoptotic or antiapoptotic depending on the cell type or subcellular localization [6]. Recent findings highlight a role for active GSK3β in cancer stem cell maintenance [7], reinforcing the interest for GSK3β inhibitors in cancer treatment.

We have previously shown that 4HPR and CDDO-Me induce tumor cell death by ATP depletion and mitochondrial bioenergetic failure leading to necrosis-like death, associated with inhibition of basal or insulin-like growth factor-1 (IGF-1)–induced AKT phosphorylation and disruption of IGF-1 survival function [8–10]. Here, we investigated modulation of GSK3β phosphorylation and antioxidant enzyme expression, in particular heme oxygenase-1 (HO-1), and poly(ADP-ribose) polymerase (PARP) cleavage as a sign of apoptosis, in the same responsive cellular models under pharmacologic redox stress. Our results show that the redox imbalance induced by 4HPR and other redox drugs in retinoblastoma Y79 cells and by CDDO-Me and 4HPR in human prostate cancer cells is associated with increased Ser9 phosphorylation of GSK3β requiring glucose metabolism and results in activation of a defense response involving the induction of HO-1, GSH, and nicotinamide adenine dinucleotide (phosphate) (NAD(P)H) [11] levels. Remarkably, GSK3 gene silencing, or expression of the GSK3β-S9A mutant, decreased HO-1 induction in CDDO-Me–treated cells. These findings highlight a correlation between GSK3β Ser9 phosphorylation and the antioxidant response, suggesting that redox stress induced by either oxido-reductive or metabolic perturbation uses a redox code that targets sensitive signaling pathways. The regulatory network described here suggests that curtailing the energy demanding antioxidant response could increase the efficacy of redox anticancer drugs.

Materials and Methods

Cell Cultures and Reagents

Human retinoblastoma Y79 cells (ATCC HTB-18), androgen-independent PC3 (ATCC CRL-1435), and DU145 (ATCC HTB-81) human prostate adenocarcinoma cells were obtained from American Type Culture Collection (ATCC) (Manassas, VA) and certified by the Interlab Cell Line Collection of the Biological Bank and Cell Factory core facility (member of the European BioBanking and Molecular Resources Research Infrastructure), IRCCS AOU S. Martino-IST, (Genoa, Italy). The cells were propagated in RPMI 1640 supplemented with either 15% (retinoblastoma cells) or 10% (prostate cancer cells) heat-inactivated FBS and 2 mM glutamine. For adherent cultures, retinoblastoma cells were

seeded on poly-D-lysine–coated dishes for 24 hours and then transferred to a chemically defined N1 medium (Invitrogen, Life Technologies, Monza, Italy). 4HPR was kindly provided by Dr James A. Crowell, Division of Cancer Prevention, National Cancer Institute (Bethesda, MD) and Dr Gregg Bullard, McKessonBio (Rockville, MD). Cells were treated with 4HPR dissolved in ethanol in a 10 mM stock solution. Human recombinant IGF-1 (PeproTech EC, London, United Kingdom) was diluted in 0.1 N acetic acid and used at the final concentration of 10 to 100 ng/ml. In the experiments with IGF-1, the cells were maintained for 24 hours in N1 defined medium without insulin. The synthetic triterpenoid CDDO-Me was kindly provided by Dr Michael B. Sporn (Dartmouth Medical School, Hanover, NH). The following reagents used were purchased from Sigma-Aldrich (Milano, Italy): the antioxidants N-acetylcysteine (NAC), desferrioxamine mesylate (DFX), and GSH ethyl ester (GSH-EE), the oxidants As_2O_3, PEITC, and DL-buthionine-[S,R]-sulfoximine, and the mitogen-activated protein kinase kinase (MEK) inhibitor bis[amino [(2-aminophenyl)thio]methylene]butanedinitrile (U0126) from BIO-MOL (Plymouth Meeting, PA); the p90 ribosomal S6 kinase (p90RSK) inhibitor BI-D1780 was provided by Dario R. Alessi (MRC Protein Phosphorylation Unit, University of Dundee, Scotland, United Kingdom). All pretreatments with antioxidants (NAC, DFX, and GSH-EE) or other reagents were carried out for 2 hours before drug administration.

Cell Viability and Cytotoxicity Assays

Cell viability was evaluated by the 3-(4,5-dimethylthiazol-2-yl)-2,5-diphenyltetrazolium bromide (MTT) assay, by lactate dehydrogenase release and ATP levels as previously described [8–10]. The absorbance was determined with a microtiter plate reader (Molecular Devices Corp, Sunnyvale, CA). Detection of cell membrane integrity was also performed by propidium iodide staining (1 μg/ml) and flow cytometry as previously described [9]. Analysis was performed on 10,000 gated cells to exclude cell debris using a CyAn ADP flow cytometer (Beckman Coulter, Milano, Italy).

Total and Reduced GSH Determination

Total GSH (reduced GSH plus glutathione disulfide (GSSG)) was determined by the enzymatic recycling method with 5,5'-dithiobis-(2-nitrobenzoic acid) (DTNB) (Ellman's reagent) (BioxyTech GSH-400 colorimetric assay; OxisResearch, Portland, OR). Total protein content was determined before metaphosphoric acid precipitation by the DC Protein Assay (Bio-Rad, Milano, Italy). Total GSH content was calculated as nanomoles per milligram of protein and expressed as percent relative to controls. Determination of GSH with monochlor-obimane (mBCl; Molecular Probes, Life Technologies; 200 nM, 37°C for 1 hour) was carried out in cells suspended in cold phosphate-buffered saline using a microplate spectrofluorometer (SpectraMax Gemini XPS; Molecular Devices) or by flow cytometry [12].

Reactive Oxygen Species Detection

The cells were incubated with 5 μM carboxymethyl dichlorofluorescin diacetate (CM-H2DCFDA) (Molecular Probes) 20 minutes before the end of treatments and analyzed by flow cytometry as described [8,9].

Determination of Glucose Uptake

Glucose uptake was determined with the hydrolyzable fluorescent probe (2-(N-(7-nitrobenz-2-oxa-1,3-diazol-4-yl)amino)-2-deoxy-D-glucose (2-NBDG) and the nonhydrolyzable 6-NBDG (Molecular

Probes) [13]. The cells were incubated with the reagents (100 μM) for 15 minutes and analyzed by flow cytometry in serum-free, phenol red–free RPMI.

Determination of Glucose-6-Phosphate Dehydrogenase Activity and NAD(P)H

The kinetics of glucose-6-phosphate dehydrogenase (G6PD) activity was determined spectrophotometrically as previously described [14]. Cytosolic NAD(P)H levels in intact cells were determined according to the method described by Rathmell et al. [11] adapted for flow cytometry.

Western Blot Analysis of Proteins

Total cell lysates were prepared with the Mammalian Cell Extraction kit (MBL, Watertown, MA), supplemented with 1 mM sodium orthovanadate. Protein quantification was performed with the DC Protein Assay (Bio-Rad). Forty micrograms of total cellular proteins was resolved on 12.5% sodium dodecyl sulfate–polyacrylamide gels and transferred on polyvinylidene difluoride membranes (GE Healthcare, Milan, Italy). The following antibodies were used: phospho–AKT-1 (Ser473), AKT, phospho-GSK3β (pGSK3β; Ser9), GSK3β, phospho–5′ adenosine monophosphate (AMP)-activated protein kinase (pAMPK; Thr172), AMPK, full-length 116-kDa and 89-kDa cleavage fragment of PARP (Asp214), phospho-ERK1/2, ERK1/2, Nrf2 (all from Cell Signaling Technology, Beverly, MA); HO-1, GSH peroxidase, Cu/Zn superoxide dismutase (SOD), G6PD (Stressgen, Enzo Life Sciences, Milano, Italy); glutamate-cysteine ligase, catalytic subunit (GCLC) (Abnova, c/o EMBL Enterprise Management Technology Transfer GmbH (EMBLEM), Heidelberg, Germany); HRP-conjugated anti-glyceraldehyde 3-phosphate dehydrogenase (GAPDH) (Novus Biologicals Inc., Littleton, CO); secondary HRP-labeled antibodies (Cell Signaling Technology). The ECL-Plus reagent was from GE Healthcare.

Immunohistochemistry

Immunohistochemical analysis was carried out on formalin-fixed, paraffin-embedded 3-μm sections of prostate biopsies provided by the Pathology Unit of our Institute. Citrate buffer (pH 6) was used for antigen unmasking; endogenous peroxidase was inactivated by 3% H_2O_2, and unspecific binding sites were blocked with goat serum. Anti-pGSK3β (Cell Signaling Technology) and HO-1 (Stressgen) antibodies were used at 10 μg/ml concentration and the reaction was revealed with the anti-rabbit HRP-DAB Plus Ultravision Detection System (Thermo Fisher Scientific, Freemont, CA).

RNA Interference and GSK3β Transfection

SignalSilence GSK3α/β target-specific and non-targeted control small interfering RNAs (siRNAs) (Cell Signaling Technology) were used to inhibit GSK3α/β as described [10]. The non-phosphorylatable hemagglutinin–GSK3β-S9A pcDNA3 (Plasmid 14754; Addgene, Cambridge, MA) was provided by Jim Woodgett (Mount Sinai Hospital, Toronto, Canada) [15]. PC3 and DU145 cells were transfected with the TransIT-TKO Transfection Reagent provided by Mirus Bio, Corp (Madison, WI), kept in the presence of gentamicin (800 μg/ml) for 15 days, and analyzed at intervals during the selection process.

Statistical Analysis

The statistical significance between two data sets expressed as means ± SD was determined by a two-tailed unpaired Student's t test using the PRISM GraphPad software. One-way analysis of variance followed by Tukey-Kramer test was used in the analysis of three or more data sets. P values were set as follows: $*P < .05$, $**P < .01$, and $***P < .001$.

Results

GSK3β Ser9 Phosphorylation Correlates with Cell Death Activation

The anticancer drugs 4HPR and CDDO-Me induce tumor cell death by bioenergetic failure due to loss of mitochondrial transmembrane potential ($\Delta\psi_m$), ATP depletion, cell membrane damage, and down-regulation of the AKT survival pathway [9,10]. In this study, we explored redox stress and survival signaling in the cell death pathways induced by CDDO-Me in prostate adenocarcinoma PC3 and DU145 cells and by 4HPR in Y79 retinoblastoma cells, focusing on the role of GSK3β in these processes.

Treatment with 4HPR induced time-dependent GSK3β phosphorylation in Y79 cells that persisted at 24 hours and was coincident with extensive PARP cleavage (Figure 1), in line with activation of caspase-3, DNA fragmentation, and nuclear apoptosis in dying cells [9]. Similar to the effects of CDDO-Me in prostate cancer cells [10], 4HPR in Y79 cells induced GSK3β phosphorylation that parallels decreased AKT phosphorylation [9]. While AKT stimulation by IGF-1 was inhibited by 4HPR, GSK3β Ser9 phosphorylation was sustained (Figure 1). Perturbation of IGF-1 signaling by 4HPR correlated with the lack of effect of IGF-1 on PARP cleavage. Reactive oxygen species (ROS) elevation by 4HPR impairs cellular bioenergetics in Y79 cells, as indicated by ATP depletion and disruption of $\Delta\psi_m$ [9]. The master energy sensor AMPK can be activated during redox stress concomitant with autophagy, hypoxia, and nutrient deprivation [16]. Increased phosphorylation at Thr172 of AMPK and its substrate acyl CoA carboxylase pACC at Ser79 confirmed that GSK3β hyperphosphorylation plays a role in 4HPR-induced cell death in critical energy conditions under redox stress.

GSK3β Ser9 Phosphorylation Is Associated with an Antioxidant Response

GSK3β phosphorylation has been associated with cytoprotective mechanisms to preserve homeostasis during metabolic stress [6]. Since 4HPR and CDDO-Me can kill tumor cells by redox stress
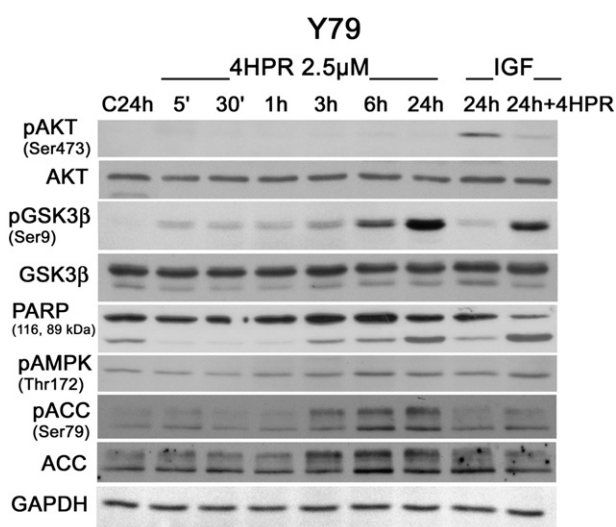

Figure 1. 4HPR sustains GSK3β Ser9 phosphorylation in Y79 cells. GSK3β phosphorylation correlates with PARP cleavage and AMPK activation in cell death induced by 4HPR (2.5 μM). IGF-1 (100 ng/ml) does not affect PARP cleavage. 4HPR inhibits IGF-1–induced AKT phosphorylation at 24 hours.

[3,9], we asked whether GSK3β phosphorylation correlates with an increased expression of antioxidant enzymes. HO-1 catalyzes the rate-limiting step in heme catabolism as an adaptive response to oxidative injury. Cytosolic Cu/Zn SOD serves to detoxify ROS. G6PD, the limiting enzyme of the pentose phosphate pathway (PPP), provides reducing equivalents (NADPH). GSH peroxidase detoxifies peroxides through GSH oxidation. Expression of all four pro-survival molecules was upregulated in 4HPR-treated Y79 cells at 24 hours (Figure 2A). Dose-dependent HO-1 and Cu/Zn SOD expression were induced in a limited concentration range, declining with the severity of cell damage

(Figure 2B) [9]. GSK3β can regulate the activity of the transcription factor Nrf2, which in turn controls the expression of G6PD, HO-1, and enzymes of GSH metabolism [17]. Indeed, Nrf2 was increased within a defined range of concentrations and declined at higher doses of 4HPR in Y79 cells (Figure 2B). Due to the potential clinical application of HO-1 pharmacological targeting [18], we limited further analysis to this enzyme. Oxidative stress triggered by 4HPR in prostate tumor cells has been extensively studied [19]; however, the antioxidant response was not explored. In PC3 cells, 4HPR (10 μM) induced time-dependent HO-1 expression and GSK3β phosphorylation, along with PARP
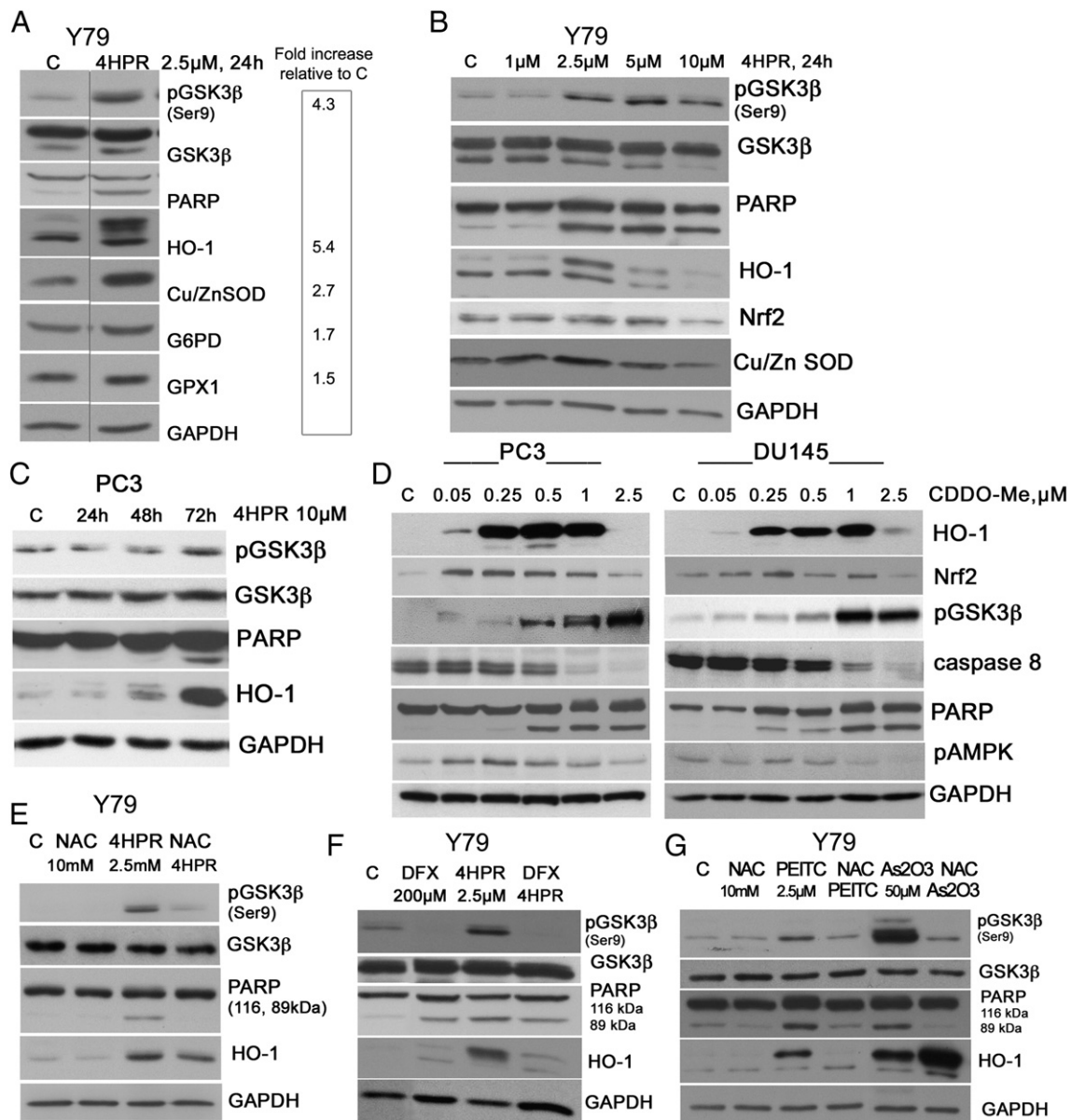

Figure 2. (A) Induction of antioxidant enzymes is associated with PARP cleavage induced by 4HPR in Y79 cells. Densitometric analysis was carried out by normalizing protein expression *versus* GAPDH and calculation of fold increase over control samples. The dividing vertical line indicates the junction between control and lanes spliced from the blot. (B) Dose-dependent increase of GSK3β phosphorylation and HO-1 and Nrf2 expression in 4HPR-treated Y79 cells. (C) Time-dependent GSK3β phosphorylation, HO-1 expression, and PARP processing in PC3 cells treated with 4HPR. (D) Dose-dependent GSK3β phosphorylation, HO-1 and Nrf2 expression, PARP and caspase-8 processing in PC3 and DU145 cells treated with CDDO-Me (24 hours). pAMPK induction indicates ATP decline, in line with previous results [10]. Pretreatment for 2 hours with the antioxidant NAC (10 mM) (E) or DFX (200 μM) (F) decreases GSK3β phosphorylation, PARP cleavage, and HO-1 expression induced by 4HPR (2.5 μM, 24 hours). (G) Similar modulation by NAC of the molecular pattern analyzed under the effect of PEITC. HO-1 overexpression is visible with the combination of As₂O₃ and NAC. In all panels, results from representative experiments are shown.

cleavage (Figure 2C). In PC3 and DU145 cells, CDDO-Me induces necrotic-like death [10]. A dose-dependent increase of pGSK3β in these cells treated with CDDO-Me (Figure 2D) [10] was associated with transient HO-1 expression and pAMPK increase, both declining in late apoptotic cells showing strong caspase-8 processing (Figure 2D). In Y79 cells, CDDO-Me at relatively low dose (250-500 nM, 24 hours) caused massive cell lysis and extensive PARP cleavage indicative of severe cell damage [20], while GSK3β Ser9 phosphorylation or HO-1 expression was not induced (Figure W1A).

To assess whether oxidative stress in general stimulates GSK3β phosphorylation, we investigated the effects of different redox drugs and antioxidants. Besides 4HPR, we used the clinically relevant prooxidants PEITC (2.5 μM) [4] and As_2O_3 (50 μM) [21]. Cell viability, as assessed by ATP levels, remarkably declined in Y79 cells treated with PEITC, As_2O_3, and CDDO-Me (Figure W1B). PEITC and As_2O_3, similarly to 4HPR [9,22], increased ROS in Y79 cells (Figure W1C). CDDO-Me can alter redox in different tumor types [23]; however, it did not increase ROS in Y79 or in PC3 cells (Figure W1, C and D). The antioxidant NAC (10 mM) that provides L-cysteine released by esterases for GSH synthesis and the iron chelator DFX (200 μM) [9,24], which both prevented mitochondrial and lysosomal damage in Y79 cells [9], effectively lowered GSK3β phosphorylation and HO-1 expression, as well as PARP cleavage, induced by 4HPR in Y79 cells (2.5 μM, 24 hours; Figure 2, E and F). Limited PARP cleavage by DFX alone has been associated with cytoprotective preconditioning in neuronal cells [25]. PEITC (2.5 μM) [4] and As_2O_3 (50 μM) [21] stimulated GSK3β Ser9 phosphorylation and PARP cleavage in Y79 cells at 24 hours (Figure 2G). This effect was prevented by NAC, which also abrogated HO-1 expression induced by PEITC in Y79 cells but further increased HO-1 expression induced by As_2O_3 (Figure 2G). This paradoxical effect could be due to the particular chemistry of reaction between GSH and trivalent arsenic, producing arsenic radicals and GSH-arsenic conjugates that inhibit GSH reductase (GR), blocking regeneration of oxidized GSH [26]. Enhanced HO-1 expression by As_2O_3 in combination with other antioxidants has been reported [27]. In contrast, PEITC and its bioactivation products form GSH conjugates that do not apparently inhibit GR [26,28]. Taken together, these data suggest that GSK3β Ser9 phosphorylation occurs during acute redox imbalance triggering cell death [9,10] and correlates with activation of a transient antioxidant defense.

Redox Imbalance Affecting GSK3β Ser9 Phosphorylation Involves ROS and GSH

Prevention of PARP cleavage induced by 4HPR, As_2O_3, and PEITC by NAC in Y79 cells (Figure 2) prompted us to investigate whether redox stress affecting GSK3β was associated with altered GSH metabolism. Determination of reduced GSH with the fluorescent probe mBCl [12] and flow cytometry analysis revealed discrete subpopulations in Y79 cells, differing in size and structural complexity (Figure 3, A and B). They were distinguished by different mBCl mean fluorescence intensity (MFI; bright and dim fluorescence cells, corresponding to about 50% and 25% of all gated cells, respectively), as confirmed by fluorescence microscopy (Figure 3A, right). A percentage of non-fluorescent cells (about 10% of the gated population) represented neuronal precursors undergoing spontaneous death upon differentiation [29] (Figure 3, A, left, and B). DL-Buthionine-[S,R]-sulfoximine was used as control to test GSH depletion. The existence of heterogeneous populations with different levels of GSH in tumors and in cell lines has been reported [30]. The

MFI of the bright fluorescence population at 24 hours after 4HPR administration was transiently elevated over controls (Figure 3C). Interestingly, GSH increase at 24 hours in the bright population was consistent with bell-shaped ROS kinetics that peaked at 6 hours and progressively declined at 24 hours after 4HPR administration [9]. These data are in line with a transient adaptive increase of GSH that can be associated with a biphasic response to lethal oxidative stress [31]. The fraction of bright fluorescent cells declined in a dose- and time-dependent manner, shifting in the dim and non-fluorescent dying population (Figure 3B; data at 16 hours of treatment are not shown). Thus, total GSH levels in the whole cell population treated with 5 μM 4HPR was decreased to approximately 50% of controls at 24 hours (average decrease of 50.2 ± 10.6%; Figure 3D).

A significant reduction of total GSH (reduced GSH plus GSSG), as determined with DTNB, was observed in Y79 cells after 24 hours of treatment with 2.5 μM 4HPR (40.8 ± 0.5% of control; mean GSH levels in controls were 10.16 ± 1.82 nmol/mg protein; Figure 3E), confirming the data obtained with mBCl (Figure 3D). In the cells pretreated with NAC (10 mM, 2 hours), intracellular total GSH was elevated over controls, both in the absence or presence of 4HPR (Figure 3E), as expected. Lack of effect of methionine to inhibit GSH efflux [32] excluded that GSH decline was due to extracellular release (data not shown). As_2O_3 and CDDO-Me substantially depleted GSH levels in Y79 cells, in contrast with PEITC that did not exert significant effects (Figure W2A). In PC3 and DU145 prostate tumor cells, GSH was significantly decreased by CDDO-Me at 24 hours of treatment (Figure W2B).

The Y79 bright and dim fluorescence populations were collected by cell sorting. The bright population showed increased basal as well as 4HPR-induced GSK3β phosphorylation relative to the total population and was able to cleave PARP in response to 4HPR (2.5 μM, 24 hours; Figure W2C). To assess whether intracellular GSH content could influence GSK3β phosphorylation, we treated the cells with a cell permeable GSH-EE (10 mM) for 16 and 24 hours. Cells treated with GSH-EE showed increased basal GSK3β phosphorylation, consistent with the previous result. In contrast, PARP cleavage, HO-1 expression (Figure W2D), and ROS induced by 2.5 μM 4HPR (Figure W2E) were decreased, indicating antioxidant effects similar to NAC. It is possible that NAC, also capable of influencing energy metabolism [33], exerts a more tunable effect on redox balance, while an abrupt uptake of GSH-EE could result in reductive stress in Y79 cells [34]. Taken together, these data suggest that GSK3β phosphorylation can signal redox perturbations, including variation in GSH levels, away from the equilibrium state.

4HPR-Resistant Cells Show Elevated GSH Levels and Enhanced GSK3β Phosphorylation

To clarify the function of GSK3β in redox stress, we analyzed GSK3β phosphorylation in established 4HPR-resistant cells. Y79, PC3, and DU145 cells surviving chronic administration of 4HPR starting from 1 μM and progressively reaching the 2.5 to 5 μM concentration range were isolated from long-term cultures and cloned by limiting dilution (Figures 4 and W3) [22]. Y79 cells resistant to 2.5 μM 4HPR (Y79-R2.5) showed significantly limited damage induced by 4HPR, as evaluated by MTT reduction and extracellular lactate dehydrogenase (Figure W3, A and B) and PARP cleavage (Figure 4A) relative to the wild-type (wt) cells. Basal GSK3β phosphorylation was enhanced, while HO-1 expression was not elevated over wt cells, suggesting a minor role for HO-1 in 4HPR resistance in Y79 cells (Figure 4A). GSH and NAD(P)H were
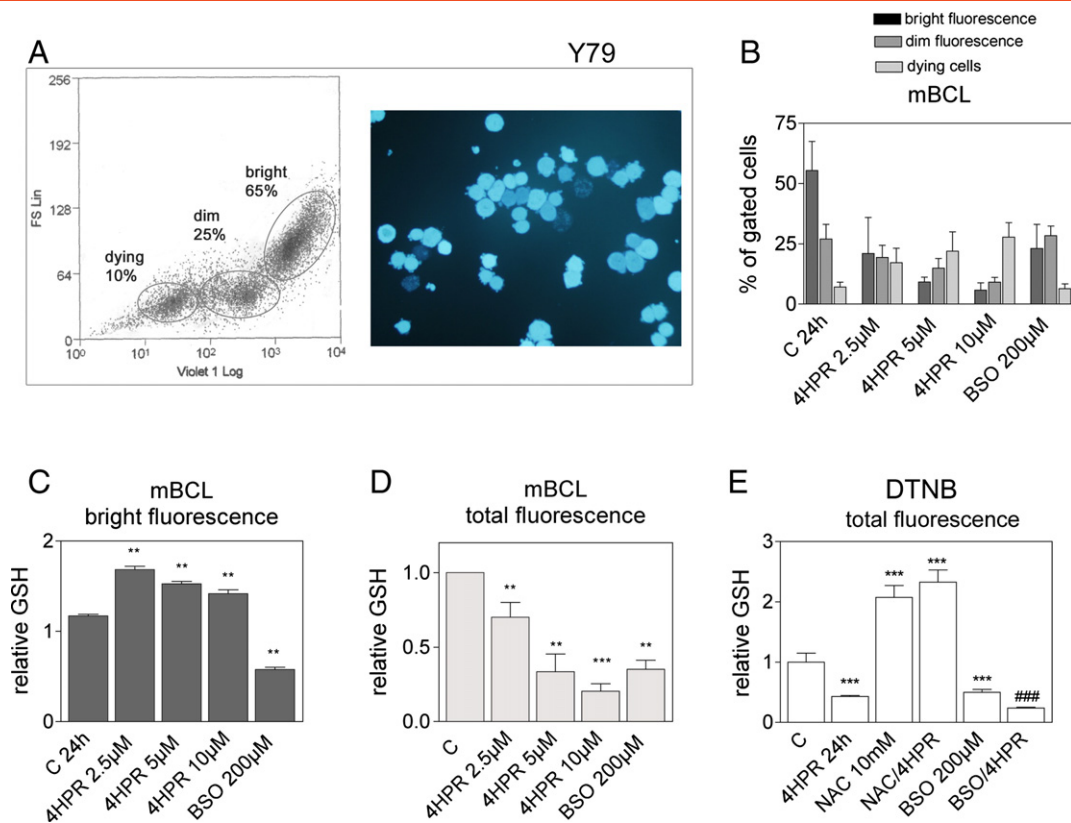
Figure 3. (A) Determination of GSH with mBCl distinguishes Y79 cell subpopulations with different GSH content. Representative flow cytometry histogram of cell subpopulations (bright fluorescence, dim fluorescence, and dying cells; left) and fluorescence microscope image (right). The analysis of mBCl fluorescence was done on 10,000 gated cells. (B) The percentage of subpopulations as mean $\pm$ SD was calculated from three independent experiments run in duplicate. (C) Relative GSH content in the bright fluorescence population at 24 hours. (D) Relative GSH in the whole-cell population at 24 hours. (E) GSH levels determined with DTNB in cells treated with 4HPR (2.5 μM, 24 hours) and effects of 2-hour pretreatment with NAC (10 mM) or CHX (0.125 μg/ml). The relative GSH content was calculated from MFI data normalized *versus* controls set as 1 from three independent experiments run in duplicate. Results are expressed as means $\pm$ SD. ***$P <$ .001 and **$P <$ .01, statistically significant difference *versus* control samples at 24 hours; ###$P <$ .001, statistically significant difference *versus* samples treated with 4HPR alone.

significantly increased in 4HPR-resistant Y79 cells cultured without 4HPR for 1 week relative to the wt cells (Figure 4B). PC3 and DU145 cells resistant to 5 μM 4HPR (PC3-R5, DU145-R5) showed increased GSK3β phosphorylation, HO-1 and GCLC expression (Figure 4, *C* and *E*, respectively), and high basal GSH and NAD(P)H levels relative to the wt cells (Figure 4, *D* and *F*), a result in line with the stabilization of a pGSK3β-mediated redox-sensitive signaling cascade in stressed PC3 and DU145 cells [10]. These data suggest that increased GSK3β phosphorylation could be part of an adaptive mechanism to tolerate long-term exposure to redox stress. This observation was corroborated by immunohistochemical analysis of human prostate tumor specimens showing elevated pGSK3β and HO-1 levels (Figure W4), in line with the evidence that oxidative stress parallels prostate tumor progression [35,36].

GSK3β Ser9 Phosphorylation Influences HO-1 Expression

To further investigate the role of GSK3β in redox remodeling, we analyzed HO-1 expression in PC3 and DU145 cells transiently transfected with an siRNA specific for GSK3α/β. Reduction of GSK3β expression has been linked to increased cellular distress in CDDO-Me–treated and untreated prostate cancer cells [10]. Since GSK3α can compensate for lack of GSK3β in some functions [37] and the role of GSK3α is poorly defined in cell death, we silenced both GSK3α and

GSK3β to better evaluate the role of GSK3 in this context. We then focused on GSK3β because of the expanding development of GSK3β pharmacologic inhibitors in clinical settings, even if isoform-specific GSK3 inhibitors are lacking. Treatment with CDDO-Me (1 μM) for 24 hours strongly induced HO-1 expression in wt and non-specific siRNA-transfected prostate cancer cells, while HO-1 was significantly decreased in GSK3β-depleted cells (Figure 5A). Similarly, transfection with the non-phosphorylatable GSK3β-S9A mutant caused a marked decline in HO-1 induction by 4HPR and CDDO-Me in the same cell lines (Figure 5, *B* and *D*), an indication that GSK3β Ser9 phosphorylation signaling is crucial to regulate HO-1 induction.

PC3 cells stably transfected with the GSK3β-S9A mutant grew slower relative to the mock-transfected cells and were more sensitive to CDDO-Me and 4HPR treatment (Figure W3D). Both PC3 and DU145 cells stably transfected with the GSK3β-S9A mutant showed elevated levels of GSH and NAD(P)H [11] relative to controls (Figure 5, *C* and *E*, respectively), suggestive of an adaptive mechanism to compensate a precarious redox balance in these cells.

Glucose Metabolism Supports GSK3β Phosphorylation Induced by Prooxidants

To resist redox stress, cells activate metabolic adaptations to feed antioxidant defenses. Since GSK3β has been shown to play a role in
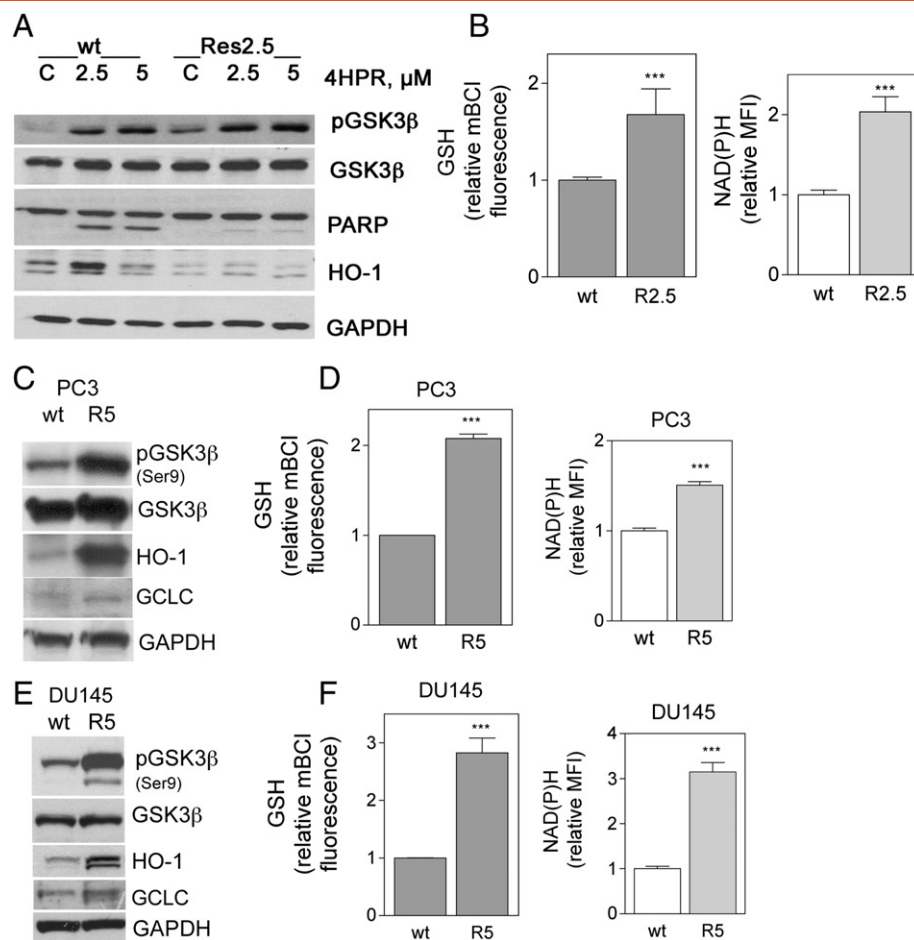
Figure 4. (A) Y79 retinoblastoma cells resistant to 4HPR show increased GSK3β phosphorylation that correlates with lack of PARP cleavage. (B) GSH and NAD(P)H levels are increased in 4HPR-resistant Y79 cells (R2.5). Increased GSK3β phosphorylation and high basal HO-1 and GCLC expression in PC3 (C) and DU145 (E) cells resistant to 4HPR (5 μM). GSH and NAD(P)H levels in PC3 (D) and DU145 (F) cells resistant to 5 μM 4HPR (R5). Data represent means ± SD from two flow cytometry analyses run in duplicate. ***$P < .001$ *versus* wt cells.

glucose-dependent survival pathways [38], we focused on glucose metabolism. The glucose antagonist 2-deoxyglucose (2DG), a non-hydrolysable glucose analog, blocks glycolysis but undergoes further metabolism through the PPP. In Y79 cells, 2DG decreased GSK3β phosphorylation and HO-1 expression during acute (24 hours) exposure to 4HPR and As$_2$O$_3$ (Figure 6, A and B). Energy loss, in particular ATP [9], in these conditions was confirmed by increased Thr172 phosphorylation of AMPK, recently implicated in NADPH balance under metabolic stress [39]. Glucose metabolism through the oxidative PPP partly contributes to NADPH homeostasis in cells under oxidative stress. As shown in Figure 2A, G6PD expression was induced in Y79 cells treated with 4HPR. Indeed, G6PD activity, after a transient up-regulation at 16 hours, declined at 24 hours after 4HPR administration (Figure 6C). Accordingly, the G6PD inhibitor 6-aminonicotinamide (6AN, 1 mM) decreased GSK3β phosphorylation and HO-1 induction by 4HPR (Figure 6D). The 89-kDa PARP cleavage fragment was decreased by 2DG and 6AN (Figure 6, A, B, and D). Anomalous regulation of PARP cleavage in caspase-independent oxidative cell death, similar to that induced by 4HPR [9], has been described [40]. These represent signs of cellular distress; both 2DG (50 mM) and 6AN (1 mM) in glucose-containing medium (5 mM glucose), alone or in combination with 4HPR, remarkably decreased MTT reduction and ATP levels in Y79 cells

(Figure 6E). In Y79 cells resistant to 4HPR, glucose metabolism, as assessed by the uptake of the glucose analogue 6-NBDG or 2-NBDG and flow cytometry, was higher relative to wt Y79 cells (Figure 6F), in line with the elevated NAD(P)H levels (Figure 4B) [11]. The lack of GSK3β phosphorylation in acutely stressed cells with impaired glucose metabolism, coupled with the enhanced requirement for glucose in 4HPR-resistant Y79 cells, suggests that GSK3β phosphorylation is glucose-dependent under stress conditions.

ERK1/2 and RSK Are Implicated in GSK3β Phosphorylation Induced by 4HPR in Y79 Cells

Phosphorylation of Ser9 on GSK3β and of Ser21 on GSK3α is mainly operated by AKT. In Y79 and prostate cancer cells, AKT phosphorylation was decreased by 4HPR and CDDO-Me, respectively, possibly due to energy depletion and redox stress [41,42] that we observed in both models [9,10] and ceramide production in the case of 4HPR [43]. We then considered other possible stress-activated pathways. GSK3 can fall under the control of ERK1/2 under oxidative stress [44–46]. The role of ERK1/2 phosphorylation in cell survival or death, depending on the duration of the signal, is well documented [45–47]. ERK1/2 phosphorylation was sustained at 24 hours after 4HPR (2.5 μM) administration in Y79 cells (Figure 7A). The MEK inhibitor UO126 decreased GSK3β
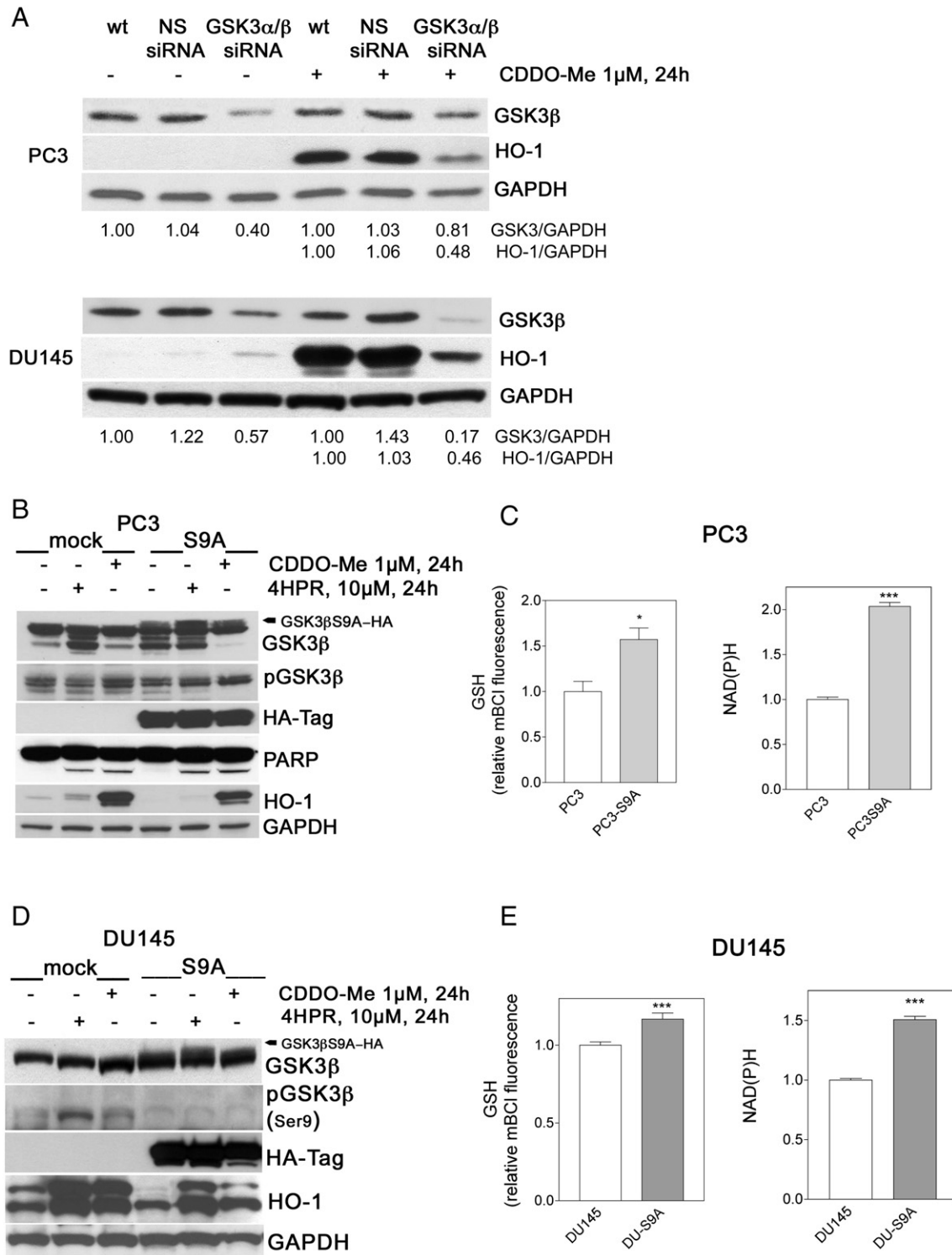
Figure 5. (A) GSK3α/β gene silencing lowers HO-1 induction by CDDO-Me (1 μM, 24 hours) in PC3 and DU145 cells. The potentiation of CDDO-Me cytotoxicity in these conditions has been published previously [10]. Optical density of bands was normalized *versus* GAPDH and fold increase expression was calculated relative to control samples set as 1. (B) Transfection with the GSK3β-S9A mutant decreases HO-1 induced by 4HPR and CDDO-Me in PC3 cells. (C) PC3 cells transfected with the GSK3β-S9A mutant show elevated levels of GSH and NAD(P)H. (D) Lower induction of HO-1 in DU145 cells transfected with the GSK3β-S9A mutant in response to 4HPR and CDDO-Me treatment. (E) Elevated GSH and NAD(P)H levels in DU145–GSK3β-S9A cells relative to the mock-transfected cells. *$P < .05$ and ***$P < .001$, statistically significant difference between GSK3β-S9A mutants and mock-transfected cells.

phosphorylation, slightly lowered HO-1 expression, and inhibited PARP cleavage (Figure 7A), suggesting a role in cell death for ERK1/2 [45]. Remarkably, UO126 rescued loss of viability and cell membrane

damage and prevented GSH decrease induced by 4HPR at 48 hours (Figure 7, *B* and *C*, respectively). Accordingly, NAC abolished ERK1/2 phosphorylation in 4HPR-treated cells (Figure 7D).
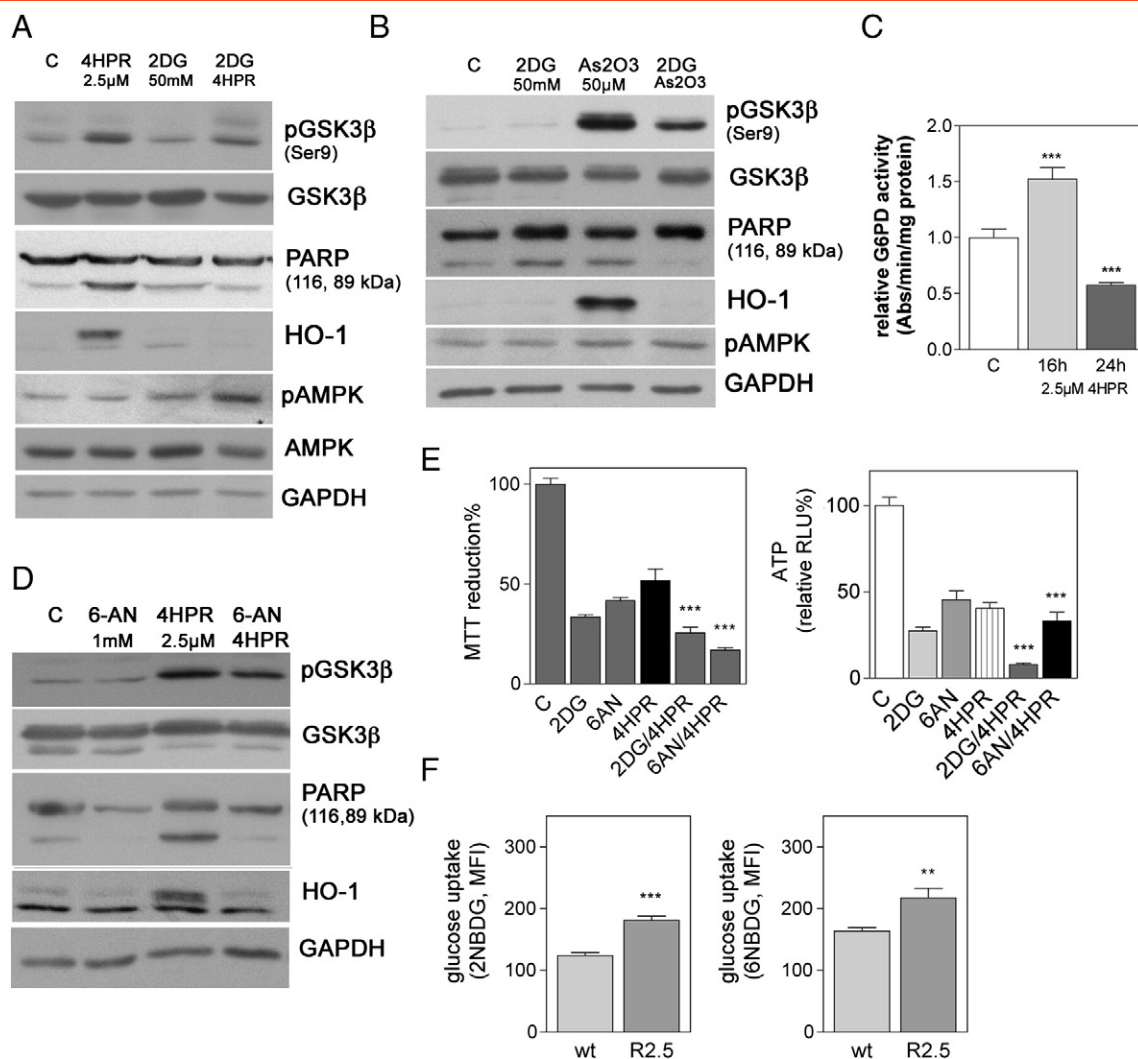
Figure 6. Interference with glucose metabolism hinders GSK3β phosphorylation induced by 4HPR and As₂O₃. (A) Y79 cells were pretreated with 2DG (50 mM) for 2 hours and then treated with 2.5 μM 4HPR for 24 hours. AMPK activation indicates energy depletion. (B) Effects of 2DG on GSK3β phosphorylation induced by As₂O₃. (C) Transient elevation at 16 hours and decreased activity of G6PD at 24 hours after 4HPR administration. Results expressed as absorbance per minute per milligram of protein were normalized relative to controls. ***$P < .001$, statistical significant differences between control and 4HPR-treated samples at 16 and 24 hours. (D) Effects of G6PD inhibition by 6AN (1 mM). (E) Decreased MTT reduction and ATP depletion in Y79 cells pretreated with 2DG or 6AN for 2 hours and treated with 4HPR for 24 hours (left). ***$P < .001$, statistically significant difference *versus* samples treated with 4HPR alone. (F) Glucose uptake, as determined with the fluorescent glucose analogue 2-NBDG or 6-NBDG and flow cytometry analysis, in wt and 4HPR-resistant Y79 cells. ***$P < .001$ and **$P < .01$.

Regulation of GSH metabolism by ERK1/2 is well documented; however, the negative or positive effects of ERK1/2 activity on GSH levels are still a matter of debate [45,46]. GSK3β can be phosphorylated at Ser9 by the stress-activated p90RSK. Phosphorylation of p90RSK can be controlled by ERK1/2 but also by other pathways including phosphatidylinositol 3-kinase and phosphoinositide-dependent kinase-1 (PDK-1) [48]. Phosphorylation at Thr356/Ser360 of RSK3, which is activated and can phosphorylate GSK3β under oxidative stress [44], was effectively elevated by 4HPR and decreased by UO126 (Figure 7A). The specific p90RSK inhibitor BI-D1780 [49] abolished 4HPR-stimulated GSK3β phosphorylation, induced PARP cleavage alone and in combination with 4HPR, abolished HO-1 induction more effectively than UO126, and increased loss of viability caused by 4HPR (Figure 7, *E* and *F*), suggesting a partially ERK1/2 independent, pro-survival role for

RSK3 in Y79 cells. The data obtained indicate that acute oxidative stress induced by 4HPR activates a signaling pathway with an ERK1/2-dependent branch mainly involved in cell death and an RSK-dependent cytoprotective branch, both converging on GSK3β phosphorylation and influencing cell fate in Y79 cells.

Discussion

In the tumor cells analyzed here, we previously described a short-term model of cell death due to bioenergetic failure [9,10]. In particular, in prostate tumor cells we demonstrated that GSK3β genetic inactivation favors necrosis and ATP loss [10]. The data obtained in this study show a relationship between GSK3β expression or phosphorylation and the modulation of the antioxidant asset of the cell, in terms of HO-1 expression and intracellular GSH, during oxidative stress. The modulation of GSK3β phosphorylation, concomitant with
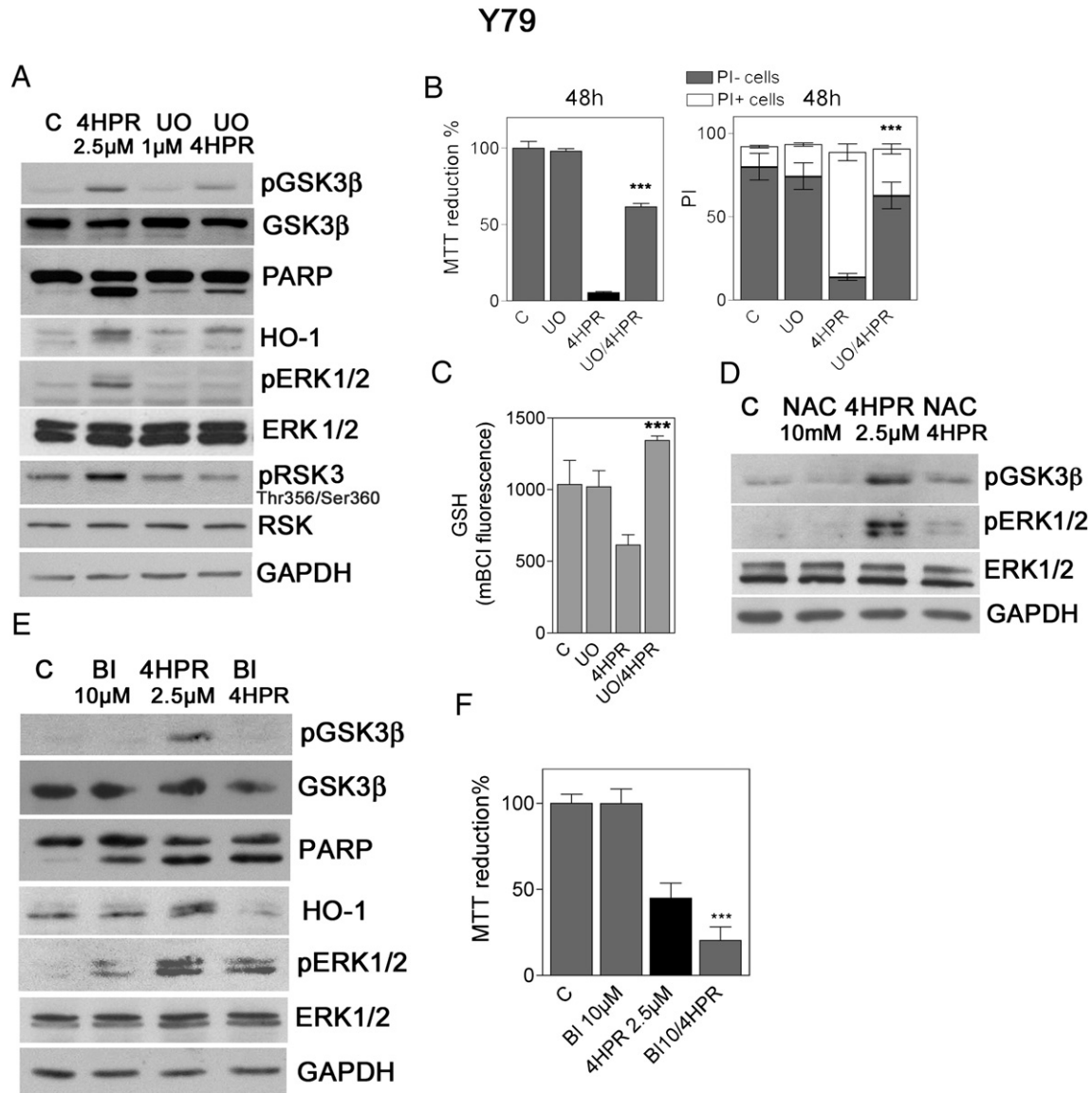
Figure 7. Analysis of signaling pathways regulating GSK3β phosphorylation in Y79 cells. (A) The MEK inhibitor UO126 decreases GSK3β phosphorylation, PARP cleavage, HO-1, and p90RSK phosphorylation induced by 4HPR at 24 hours. (B) UO126 rescues loss of MTT reduction and cell membrane damage, as measured by propidium iodide (PI) permeability, by 4HPR (2.5 μM) at 48 hours. The data shown are means ± SD of three independent experiments run in duplicate. (C) UO126 preserves GSH levels. Data were collected at 48 hours of treatment with 4HPR (2.5 μM) from three independent measurements run in duplicate. Means ± SD are shown. ***$P < .001$, statistical significance of differences *versus* samples treated with 4HPR alone. (D) The antioxidant NAC inhibits sustained ERK1/2 phosphorylation induced by 4HPR at 24 hours, an indication of redox control of ERK1/2 during oxidative stress. (E) The p90RSK inhibitor BI-D1780 inhibits GSK3β phosphorylation, but not ERK1/2 phosphorylation, suggesting GSK3β regulation by p90RSK downstream ERK1/2. (F) BI-D1780 (10 μM) exacerbates 4HPR toxicity in Y79 cells (2.5 μM, 24 hours). ***$P < .001$, statistical significance of differences *versus* samples treated with 4HPR alone.

an energy demanding antioxidant response, thus appears as coordinated processes in line with a dual role of GSK3β in cytoprotection and cell death [50]. Several lines of evidence support this suggestion: 1) Short-term genetic depletion of GSK3β by siRNA or transfection with the GSK3β-S9A mutant, both converging on deficient GSK3β Ser9 signaling, decreased HO-1 induction in cells during acute oxidative stress. 2) 4HPR-resistant retinoblastoma and prostate cancer cells, representing models of adaptation to chronic stress, showed elevated GSK3β phosphorylation, intracellular GSH, and NADPH. 3) Antioxidants prevented GSK3β phosphorylation, paralleled by inhibition of PARP cleavage, a marker of nuclear

apoptosis. 4) In bioenergetic stress models due to impaired glucose metabolism, GSK3β phosphorylation along with HO-1 expression was decreased, and 4HPR cytotoxicity was increased.

Our data indicate that GSK3β responds to an ample array of redox perturbations, however within a limited range of either oxidative or reductive equilibrium. GSK3β Ser9 phosphorylation was modulated by ROS-mediated signals in Y79 cells treated with 4HPR, PEITC, and As_2O_3, in keeping with previous observations [44,51]. In CDDO-Me–treated prostate tumor cells, where GSK3β Ser9 phosphorylation and HO-1 were induced, no ROS burst was observed; however, in these cells GSH declined, an event shared with

Y79 cells exposed to PEITC and As$_2$O$_3$. Interestingly, GSK3β responded to GSH-EE treatment, possibly sensing a disproportionate reducing milieu [34]. GSK3β might be part of a mechanism that propagates signals of mitochondrial damage, independently of ROS overproduction, coupled with thiol imbalance.

We speculate that one possible function of GSK3β is to alert defenses against redox instability and that GSK3β phosphorylation and coordinated redox changes, including HO-1 induction, promoting apoptotic cell death and delaying necrosis in acute damage (Figure W5). In fact, transient GSK3β genetic inactivation, which exacerbates cell necrosis in apoptotic cells treated with CDDO-Me [10], lowered the ability to induce HO-1. Interestingly, HO-1 expression has been shown to modulate apoptotic and necrotic cell death pathways [52,53]. In this context, the antioxidant effects of HO-1 could favor a reducing milieu required for caspase activation [54]. Further, prostate tumor cells stably transfected with the GSK3β-S9A construct competing with the endogenous GSK3β showed lower levels of HO-1 under stress. Decreased HO-1 expression in cells depleted of GSK3β or the GSK3β-S9A mutant might indicate that GSK3β Ser9–mediated signaling is a crucial event to induce HO-1. In GSK3β-S9A cells, elevated basal GSH and NADPH were suggestive of an acquired tolerance to a precarious redox equilibrium due to a pool of unphosphorylatable GSK3β-S9A during selection.

Our data indicate that modulation of GSK3β activity could help preserve a balanced milieu and bioenergetic resources in severe oxidative injury by enhancing redox cycling or stimulation of GSH metabolism. This suggestion is supported by the data indicating that acute exposure to 4HPR in Y79 cells stimulates transient elevation of GSH and G6PD activity producing NADPH. NADPH, a cofactor of GR, is provided by enhanced glucose metabolism through the PPP, feeding the main antioxidant defense of the cell [55]. In line with this, glucose metabolism inhibitors repressed GSK3β phosphorylation and activation of the antioxidant response. Most importantly, glucose uptake was enhanced in 4HPR-resistant Y79 cells, suggesting that gradual stabilization of some of the antioxidant mechanisms activated upon acute exposure was functional to the selection leading to drug resistance. In 4HPR-resistant prostate clones, GSK3β phosphorylation, GSH, NAD(P)H, and HO-1 were elevated over the wt counterparts, implying that GSK3β Ser9 phosphorylation helps adapt to chronic redox and metabolic stress.

The function of GSK3β does not appear identical in retinoblastoma Y79 and in the prostate tumor cells analyzed here. One major difference might be the lack of caspase-8 in Y79 cells. In fact, GSK3β inhibits caspase-8 [6], whose activation was enhanced by LiCl or GSK3β gene silencing in CDDO-Me–induced prostate tumor cell death [10]. Opposing roles for GSK3 in cell-specific apoptotic programs, even in the same cell type, have been described [6,56]. In non-tumor cells, GSK3β phosphorylation propagates survival signals [6], and upon oxidative stress, the change in GSK3β phosphorylation varies depending on the cell type. For example, in kidney cells oxidative injury has been shown to mitigate GSK3β phosphorylation [57]. Accordingly, GSK3β inhibitors are used in clinical trials for neurodegenerative and cardiovascular disorders [6]. In several tumor models, GSK3β has been proposed as a tumor suppressor [58,59]; in contrast, GSK3β promotes tumorigenesis and development of ovarian, colon, liver, and pancreatic carcinomas. In prostate tumor cells, GSK3β inactivation is regarded as a potential therapeutic target [6,10].

The definition of the molecular events leading to persistent GSK3β phosphorylation and related redox remodeling requires

further investigation. In Y79 cells, the result that the MEK inhibitor UO126 preserves cell viability and GSH in 4HPR-stressed cells indicates that pro-survival RSK signaling [44] is partly independent of ERK1/2 in this GSK3β-mediated regulatory network. Reciprocal regulation between GSK3β, ERK1/2, and RSK has been described [60,61] (Figure W5). In this context, hyperresponsive signaling and inadequate inactivation of ERK1/2 could contribute to the severity of cell damage; however, we cannot exclude that redox imbalance inactivates redox-sensitive protein phosphatases [62]. GSK3β has been shown to regulate Nrf2 activity, allowing up-regulation of antioxidant phase II genes including HO-1 and GSH regulators [17]. The transient induction of Nrf2 we observed is suggestive of a functional adjustment mediated by GSK3β phosphorylation, possibly by catalyzing the formation of a phosphodegron [17], to adapt GSH metabolism and HO-1 expression during acute oxidative stress.

Tumor-specific oxidative stress received attention as a promising therapeutic target [1,63]. Clinicopathologic traits of constitutive oxidative stress in retinoblastoma [64,65] have encouraged clinical studies of redox therapeutics, including As$_2$O$_3$. Chemopreventive derivatives of natural redox compounds like 4HPR, CDDO-Me, and PEITC have been shown to prompt homeostatic repair in early stages of carcinogenesis, while inducing tumor cell death [63,66]. The data presented here suggest that the energetic resources needed to counteract acute cell damage conflict with the high metabolic demand of frank tumor cells, eventually leading to tumor cell death. In contrast, adaptation to chronic stress in drug-resistant cells stably engages some of the same homeostatic antioxidant mechanisms (Figure W5). Cell stress evokes interweaved events, after which the severity of damage or successful channeling of cytoprotective signaling and effector mechanisms prevails. In this context, our novel observations on drug resistance assign a role for GSK3β in redox remodeling to determine cell fate.

Supplementary data to this article can be found online at http://dx.doi.org/10.1016/j.neo.2014.07.012.

Acknowledgements

References

[1] Trachootham D, Alexandre J, and Huang P (2009). Targeting cancer cells by ROS-mediated mechanisms: a radical therapeutic approach? *Nat Rev Drug Discov* **8**, 579–591.

[2] Sogno I, Venè R, Sapienza C, Ferrari N, Tosetti F, and Albini A (2009). Anti-angiogenic properties of chemopreventive drugs: fenretinide as a prototype. *Recent Results Cancer Res* **181**, 71–76.

[3] Liby KT, Yore MM, and Sporn MB (2007). Triterpenoids and rexinoids as multifunctional agents for the prevention and treatment of cancer. *Nat Rev Cancer* **7**, 357–369.

[4] Trachootham D, Zhou Y, Zhang H, Demizu Y, Chen Z, Pelicano H, Chiao PJ, Achanta G, Arlinghaus RB, and Liu J, et al (2006). Selective killing of

oncogenically transformed cells through a ROS-mediated mechanism by beta-phenylethyl isothiocyanate. *Cancer Cell* **10**, 241–252.

[5] Schieber M and Chandel NS (2014). ROS function in redox signaling and oxidative stress. *Curr Biol* **24**, R453-462.

[6] Beurel E and Jope RS (2006). The paradoxical pro- and anti-apoptotic actions of GSK3 in the intrinsic and extrinsic apoptosis signaling pathways. *Prog Neurobiol* **79**, 173–189.

[7] Huang J, Zhang Y, Bersenev A, O'Brien WT, Tong W, Emerson SG, and Klein PS (2009). Pivotal role for glycogen synthase kinase-3 in hematopoietic stem cell homeostasis in mice. *J Clin Invest* **119**, 3519–3529.

[8] Tosetti F, Vene R, Arena G, Morini M, Minghelli S, Noonan DM, and Albini A (2003). *N*-(4-hydroxyphenyl)retinamide inhibits retinoblastoma growth through reactive oxygen species-mediated cell death. *Mol Pharmacol* **63**, 565–573.

[9] Venè R, Arena G, Poggi A, D'Arrigo C, Mormino M, Noonan DM, Albini A, and Tosetti F (2007). Novel cell death pathways induced by *N*-(4-hydroxyphenyl)retinamide: therapeutic implications. *Mol Cancer Ther* **6**, 286–298.

[10] Venè R, Larghero P, Arena G, Sporn MB, Albini A, and Tosetti F (2008). Glycogen synthase kinase 3β regulates cell death induced by synthetic triterpenoids. *Cancer Res* **68**, 6987–6996.

[11] Rathmell JC, Fox CJ, Plas DR, Hammerman PS, Cinalli RM, and Thompson CB (2003). Akt-directed glucose metabolism can prevent Bax conformation change and promote growth factor-independent survival. *Mol Cell Biol* **23**, 7315–7328.

[12] Rice GC, Bump EA, Shrieve DC, Lee W, and Kovacs M (1986). Quantitative analysis of cellular glutathione by flow cytometry utilizing monochlorobimane: some applications to radiation and drug resistance in vitro and in vivo. *Cancer Res* **46**, 6105–6110.

[13] Aller CB, Ehmann S, Gilman-Sachs A, and Snyder AK (1997). Flow cytometric analysis of glucose transport by rat brain cells. *Cytometry* **27**, 262–268.

[14] Ursini MV, Parrella A, Rosa G, Salzano S, and Martini G (1997). Enhanced expression of glucose-6-phosphate dehydrogenase in human cells sustaining oxidative stress. *Biochem J* **323**(Pt 3), 801–806.

[15] Stambolic V and Woodgett JR (1994). Mitogen inactivation of glycogen synthase kinase-3β in intact cells via serine 9 phosphorylation. *Biochem J* **303**(Pt 3), 701–704.

[16] Cardaci S, Filomeni G, and Ciriolo MR (2013). Redox implications of AMPK-mediated signal transduction beyond energetic clues. *J Cell Sci* **125**, 2115–2125.

[17] Rada P, Rojo AI, Evrard-Todeschi N, Innamorato NG, Cotte A, Jaworski T, Tobon-Velasco JC, Devijver H, Garcia-Mayoral MF, and Van Leuven F, et al (2012). Structural and functional characterization of Nrf2 degradation by the glycogen synthase kinase 3/β-TrCP axis. *Mol Cell Biol* **32**, 3486–3499.

[18] Calabrese V, Cornelius C, Dinkova-Kostova AT, Calabrese EJ, and Mattson MP (2010). Cellular stress responses, the hormesis paradigm, and vitagenes: novel targets for therapeutic intervention in neurodegenerative disorders. *Antioxid Redox Signal* **13**, 1763–1811.

[19] Hail Jr N, Chen P, and Kepa JJ (2009). Selective apoptosis induction by the cancer chemopreventive agent *N*-(4-hydroxyphenyl)retinamide is achieved by modulating mitochondrial bioenergetics in premalignant and malignant human prostate epithelial cells. *Apoptosis* **14**, 849–863.

[20] Bentele M, Lavrik I, Ulrich M, Stösser S, Heermann DW, Kalthoff H, Krammer PH, and Eils R (2004). Mathematical modeling reveals threshold mechanism in CD95-induced apoptosis. *J Cell Biol* **166**, 839–851.

[21] Duyndam MC, Hulscher TM, Fontijn D, Pinedo HM, and Boven E (2001). Induction of vascular endothelial growth factor expression and hypoxia-inducible factor 1α protein by the oxidative stressor arsenite. *J Biol Chem* **276**, 48066–48076.

[22] Benelli R, Monteghirfo S, Venè R, Tosetti F, and Ferrari N (2010). The chemopreventive retinoid 4HPR impairs prostate cancer cell migration and invasion by interfering with FAK/AKT/GSK3β pathway and β-catenin stability. *Mol Cancer* **9**, 142.

[23] Ikeda T, Sporn M, Honda T, Gribble GW, and Kufe D (2003). The novel triterpenoid CDDO and its derivatives induce apoptosis by disruption of intracellular redox balance. *Cancer Res* **63**, 5551–5558.

[24] Persson HL, Yu Z, Tirosh O, Eaton JW, and Brunk UT (2003). Prevention of oxidant-induced cell death by lysosomotropic iron chelators. *Free Radic Biol Med* **34**, 1295–1305.

[25] Garnier P, Ying W, and Swanson RA (2003). Ischemic preconditioning by caspase cleavage of poly(ADP-ribose) polymerase-1. *J Neurosci* **23**, 7967–7973.

[26] Thomas DJ (2009). Unraveling arsenic—glutathione connections. *Toxicol Sci* **107**, 309–311.

[27] Diaz Z, Colombo M, Mann KK, Su H, Smith KN, Bohle DS, Schipper HM, and Miller Jr WH (2005). Trolox selectively enhances arsenic-mediated oxidative stress and apoptosis in APL and other malignant cell lines. *Blood* **105**, 1237–1245.

[28] Yoshigae Y, Sridar C, Kent UM, and Hollenberg PF (2013). The inactivation of human CYP2E1 by phenethyl isothiocyanate, a naturally occurring chemopreventive agent, and its oxidative bioactivation. *Drug Metab Dispos* **41**, 858–869.

[29] Raff MC, Barres BA, Burne JF, Coles HS, Ishizaki Y, and Jacobson MD (1993). Programmed cell death and the control of cell survival: lessons from the nervous system. *Science* **262**, 695–700.

[30] Shrieve DC, Bump EA, and Rice GC (1988). Heterogeneity of cellular glutathione among cells derived from a murine fibrosarcoma or a human renal cell carcinoma detected by flow cytometric analysis. *J Biol Chem* **263**, 14107–14114.

[31] Kirkland RA and Franklin JL (2001). Evidence for redox regulation of cytochrome C release during programmed neuronal death: antioxidant effects of protein synthesis and caspase inhibition. *J Neurosci* **21**, 1949–1963.

[32] Meredith MJ, Cusick CL, Soltaninassab S, Sekhar KS, Lu S, and Freeman ML (1998). Expression of Bcl-2 increases intracellular glutathione by inhibiting methionine-dependent GSH efflux. *Biochem Biophys Res Commun* **248**, 458–463.

[33] Wu CA, Chao Y, Shiah SG, and Lin WW (2013). Nutrient deprivation induces the Warburg effect through ROS/AMPK-dependent activation of pyruvate dehydrogenase kinase. *Biochim Biophys Acta* **1833**, 1147–1156.

[34] Zhang H, Limphong P, Pieper J, Liu Q, Rodesch CK, Christians E, and Benjamin IJ (2012). Glutathione-dependent reductive stress triggers mitochondrial oxidation and cytotoxicity. *FASEB J* **26**, 1442–1451.

[35] Kumar B, Koul S, Khandrika L, Meacham RB, and Koul HK (2008). Oxidative stress is inherent in prostate cancer cells and is required for aggressive phenotype. *Cancer Res* **68**, 1777–1785.

[36] Freitas M, Baldeiras I, Proenca T, Alves V, Mota-Pinto A, and Sarmento-Ribeiro A (2012). Oxidative stress adaptation in aggressive prostate cancer may be counteracted by the reduction of glutathione reductase. *FEBS Open Bio* **2**, 119–128.

[37] Doble BW, Patel S, Wood GA, Kockeritz LK, and Woodgett JR (2007). Functional redundancy of GSK-3α and GSK-3β in Wnt/β-catenin signaling shown by using an allelic series of embryonic stem cell lines. *Dev Cell* **12**, 957–971.

[38] Zhao Y, Altman BJ, Coloff JL, Herman CE, Jacobs SR, Wieman HL, Wofford JA, Dimascio LN, Ilkayeva O, and Kelekar A, et al (2007). Glycogen synthase kinase 3α and 3β mediate a glucose-sensitive antiapoptotic signaling pathway to stabilize Mcl-1. *Mol Cell Biol* **27**, 4328–4339.

[39] Jeon SM, Chandel NS, and Hay N (2012). AMPK regulates NADPH homeostasis to promote tumour cell survival during energy stress. *Nature* **485**, 661–665.

[40] Erdélyi K, Bakondi E, Gergely P, Szabó C, and Virág L (2005). Pathophysiologic role of oxidative stress-induced poly(ADP-ribose) polymerase-1 activation: focus on cell death and transcriptional regulation. *Cell Mol Life Sci* **62**, 751–759.

[41] Zhang HH, Lipovsky AI, Dibble CC, Sahin M, and Manning BD (2006). S6K1 regulates GSK3 under conditions of mTOR-dependent feedback inhibition of Akt. *Mol Cell* **24**, 185–197.

[42] Tzatsos A and Tsichlis PN (2007). Energy depletion inhibits phosphatidylinositol 3-kinase/Akt signaling and induces apoptosis via AMP-activated protein kinase-dependent phosphorylation of IRS-1 at Ser-794. *J Biol Chem* **282**, 18069–18082.

[43] Hail Jr N, Kim HJ, and Lotan R (2006). Mechanisms of fenretinide-induced apoptosis. *Apoptosis* **11**, 1677–1694.

[44] Nemoto S, Takeda K, Yu ZX, Ferrans VJ, and Finkel T (2000). Role for mitochondrial oxidants as regulators of cellular metabolism. *Mol Cell Biol* **20**, 7311–7318.

[45] Luo Y and DeFranco DB (2006). Opposing roles for ERK1/2 in neuronal oxidative toxicity: distinct mechanisms of ERK1/2 action at early versus late phases of oxidative stress. *J Biol Chem* **281**, 16436–16442.

[46] Chen ZH, Saito Y, Yoshida Y, Noguchi N, and Niki E (2008). Regulation of GCL activity and cellular glutathione through inhibition of ERK phosphorylation. *Biofactors* **33**, 1–11.

[47] Meloche S and Pouyssegur J (2007). The ERK1/2 mitogen-activated protein kinase pathway as a master regulator of the G1- to S-phase transition. *Oncogene* **26**, 3227–3239.

[48] Anjum R and Blenis J (2008). The RSK family of kinases: emerging roles in cellular signalling. *Nat Rev Mol Cell Biol* **9**, 747–758.

[49] Sapkota GP, Cummings L, Newell FS, Armstrong C, Bain J, Frodin M, Grauert M, Hoffmann M, Schnapp G, and Steegmaier M, et al (2007). BI-D1870 is a specific inhibitor of the p90 RSK (ribosomal S6 kinase) isoforms in vitro and in vivo. *Biochem J* **401**, 29–38.

[50] Luo J (2009). Glycogen synthase kinase 3β (GSK3β) in tumorigenesis and cancer chemotherapy. *Cancer Lett* **273**, 194–200.

[51] Connor KM, Subbaram S, Regan KJ, Nelson KK, Mazurkiewicz JE, Bartholomew PJ, Aplin AE, Tai YT, Aguirre-Ghiso J, and Flores SC, et al (2005). Mitochondrial H_2O_2 regulates the angiogenic phenotype via PTEN oxidation. *J Biol Chem* **280**, 16916–16924.

[52] Panahian N and Maines MD (2001). Site of injury-directed induction of heme oxygenase-1 and -2 in experimental spinal cord injury: differential functions in neuronal defense mechanisms? *J Neurochem* **76**, 539–554.

[53] Morse D, Lin L, Choi AM, and Ryter SW (2009). Heme oxygenase-1, a critical arbitrator of cell death pathways in lung injury and disease. *Free Radic Biol Med* **47**, 1–12.

[54] Pervaiz S (2006). Pro-oxidant milieu blunts scissors: insight into tumor progression, drug resistance, and novel druggable targets. *Curr Pharm Des* **12**, 4469–4477.

[55] Gillies RJ and Gatenby RA (2007). Hypoxia and adaptive landscapes in the evolution of carcinogenesis. *Cancer Metastasis Rev* **26**, 311–317.

[56] Mulholland DJ, Dedhar S, Wu H, and Nelson CC (2006). PTEN and GSK3β: key regulators of progression to androgen-independent prostate cancer. *Oncogene* **25**, 329–337.

[57] Bao H, Ge Y, Zhuang S, Dworkin LD, Liu Z, and Gong R (2012). Inhibition of glycogen synthase kinase-3β prevents NSAID-induced acute kidney injury. *Kidney Int* **81**, 662–673.

[58] Farago M, Dominguez I, Landesman-Bollag E, Xu X, Rosner A, Cardiff RD, and Seldin DC (2005). Kinase-inactive glycogen synthase kinase 3β promotes Wnt signaling and mammary tumorigenesis. *Cancer Res* **65**, 5792–5801.

[59] Leis H, Segrelles C, Ruiz S, Santos M, and Paramio JM (2002). Expression, localization, and activity of glycogen synthase kinase 3β during mouse skin tumorigenesis. *Mol Carcinog* **35**, 180–185.

[60] Wang Q, Zhou Y, Wang X, and Evers BM (2006). Glycogen synthase kinase-3 is a negative regulator of extracellular signal-regulated kinase. *Oncogene* **25**, 43–50.

[61] Ding Q, Xia W, Liu JC, Yang JY, Lee DF, Xia J, Bartholomeusz G, Li Y, Pan Y, and Li Z, et al (2005). Erk associates with and primes GSK-3β for its inactivation resulting in upregulation of β-catenin. *Mol Cell* **19**, 159–170.

[62] Levinthal DJ and Defranco DB (2005). Reversible oxidation of ERK-directed protein phosphatases drives oxidative toxicity in neurons. *J Biol Chem* **280**, 5875–5883.

[63] Sogno I, Venè R, Ferrari N, De Censi A, Imperatori A, Noonan DM, Tosetti F, and Albini A (2009). Angioprevention with fenretinide: Targeting angiogenesis in prevention and therapeutic strategies. *Crit Rev Oncol Hematol* **75**, 2–14.

[64] Kutty G, Hayden B, Osawa Y, Wiggert B, Chader GJ, and Kutty RK (1992). Heme oxygenase: expression in human retina and modulation by stress agents in a human retinoblastoma cell model system. *Curr Eye Res* **11**, 153–160.

[65] Deepa PR, Nalini V, Mallikarjuna K, Vandhana S, and Krishnakumar S (2009). Oxidative stress in retinoblastoma: correlations with clinicopathologic features and tumor invasiveness. *Curr Eye Res* **34**, 1011–1018.

[66] Tosetti F, Noonan D, and Albini A (2009). Metabolic regulation and redox activity as mechanisms for angioprevention by dietary phytochemicals. *Int J Cancer* **125**, 1993–2003.